Available online at www.sciencedirect.com
ScienceDirect
Journal of Hazardous Materials 152 (2008) 120–127
Journal of Hazardous Materials
www.elsevier.com/locate/jhazmat

Degradation of C.I. Reactive Red 2 (RR2) using ozone-based systems: Comparisons of decolorization efficiency and power consumption

Chung-Hsin Wu [a,*], How-Yong Ng [b]

[a] *Department of Environmental Engineering, Da-Yeh University, 112, Shan-Jiau Road, Da-Tsuen, Chang-Hua, Taiwan, ROC*
[b] *Division of Environmental science and Engineering, National University of Singapore, Singapore*

Received 14 April 2007; received in revised form 21 June 2007; accepted 21 June 2007
Available online 28 June 2007

Abstract

This study investigated the decolorization efficiency of C.I. Reactive Red 2 (RR2) in O_3, O_3/H_2O_2, O_3/Fe^{3+}, $O_3/H_2O_2/Fe^{3+}$, UV/O_3, $UV/O_3/Fe^{3+}$, $UV/O_3/H_2O_2$ and $UV/O_3/H_2O_2/Fe^{3+}$ systems at various pHs. The effective energy consumption constants and the electrical energy per order of pollutant removal (EE/O) were also determined. The experimental results indicated that the energy efficiency was highest at $[H_2O_2]_0 = 1000$ mg/l and $[Fe^{3+}]_0 = 25$ mg/l. Accordingly, the H_2O_2 and Fe^{3+} doses in the hybrid ozone- and UV/ozone-based systems were controlled at these values. This work suggests that the dominant reactant in O_3, O_3/Fe^{3+} and O_3/H_2O_2 systems was O_3 and that in the $O_3/H_2O_2/Fe^{3+}$ system was H_2O_2/Fe^{3+}. The experimental results revealed that the combinations of Fe^{3+} or H_2O_2/Fe^{3+} with O_3 at pH 4 and of H_2O_2 or H_2O_2/Fe^{3+} with UV/O_3 at pH 4 or 7 yielded a higher decolorization rate than O_3 and UV/O_3, respectively. At pH 4, the EE/O results demonstrated that the $UV/O_3/H_2O_2/Fe^{3+}$ system reduced 85% of the energy consumption compared with the UV/O_3 system. Moreover, the $O_3/H_2O_2/Fe^{3+}$ system reduced 62% of the energy consumption compared with the O_3 system. At pH 7, the EE/O results revealed that the $UV/O_3/H_2O_2/Fe^{3+}$ system consumed half the energy of the UV/O_3 system.

Keywords: C.I. Reactive Red 2; Ozone; Ferric; Hydrogen peroxide; Decolorization; Power consumption

1. Introduction

The textile industry utilizes numerous dyes and pigments. Among these, azo dyes represent the largest and the most important class of commercial dyes. Most commercial dyes are not directly toxic. Colored wastewater is subject to strict environmental legislation because they have a negative effect on the photosynthetic activity in Taiwan. Accordingly, decolorization of dye effluents has attracted increased attention. The C.I. Reactive Red 2 (RR2), dye with the most commonly used anchor – the dichlorotriazine group – was selected as the parent compound in this study. Conventional treatment cannot efficiently remove dyes from textile wastewater, because they are stable against light and biological degradation. Treatments such as adsorption, flotation and coagulation only perform the phase transfer of pollutants but do not destroy them. Hence, further treatments are required. Advanced oxidation processes (AOPs) are alternative methods for decolorizing and reducing recalcitrant wastewater loads from textile companies. AOPs are based on the generation of hydroxyl radicals in water, which are highly reactive and nonselective oxidants that can oxidize organic compounds. Hydroxyl radicals have an oxidation potential that exceeds that of ozone and H_2O_2 – 2.80 V for hydroxyl radicals, 2.07 V for ozone and 1.78 V for H_2O_2. Ozone may either react directly with organic compounds or decompose highly reactive species, such as hydroxyl radicals. Ozonation has potential in decolorization for the following reasons: (1) no sludge remains; (2) danger is minimal; (3) decolorization and degradation occur in one step; (4) it is easily performed; (5) little space is required, and (6) all residual ozone can be easily decomposed to oxygen and water [1]. Accordingly, the ozone-based systems are feasible for decolorizing azo dyes.

Combining various AOPs commonly causes interesting synergistic effects that can markedly reduce the reaction time and economic cost. Various studies have explored the synergistic effects of the decolorization of dyes in ozone-based systems,

* Fax: +886 55334958.
E-mail address: chunghsinwu@yahoo.com.tw (C.-H. Wu).

0304-3894/$ – see front matter © 2007 Elsevier B.V. All rights reserved.
doi:10.1016/j.jhazmat.2007.06.073

such as O_3/H_2O_2 [2–4], O_3/Fe^{2+} [5,6], $UV/O_3/H_2O_2$ [2,4,7], $O_3/H_2O_2/Fe^{2+}$ [2], $UV/O_3/Fe^{2+}$ [5,6,8], $UV/O_3/Fe^{3+}$ [9], $UV/TiO_2/O_3$ [4,10], $UV/O_3/H_2O_2/Fe^{3+}$ [4], $UV/O_3/Fe^{2+}/Cu^{2+}$ [6,8], $UV/O_3/H_2O_2/Fe^{2+}$ [2] and $UV/O_3/TiO_2/SnO_2$ [11]. Since Fe^{3+} in hybrid ozone-based systems has rarely been examined and iron catalysts are abundant in nature, this study incorporates Fe^{3+} into the hybrid ozone-based systems to evaluate the decolorization efficiency of RR2 at various pHs.

The photodegradation of aqueous organic pollutant is an electric-energy-intensive process, and electric energy typically represents a major fraction of the operating costs. Simple figures-of-merit based on electric energy consumption can therefore be very useful. The electrical energy per order of pollutant removal (EE/O) is a powerful scale-up parameter and a measure of the treatment rate in a fixed volume of contaminated water as a function of the applied specific energy dose [12]. The EE/O value was adopted to compare the energy efficiency of different systems. In the case of low-pollutant concentrations, the EE/O (kW h m^{-3} $order^{-1}$) can be determined from the following equations.

$$\mathrm{EE/O} = \frac{Pt \times 1000}{V \times 60 \times \log(A_i/A_o)} \quad (1)$$

$$\ln\left(\frac{A_i}{A_o}\right) = k_a t \quad (2)$$

where P is the power (kW) of the AOPs; t is the reaction time (min); V is the volume (l) of the water in the reactor; A_i and A_o are the inflow and outflow RR2 absorbance and k_a is the pseudo-first-order rate constant (min^{-1}) for the decay of the pollutant in the pollutant concentration [12,13]. Combining Eqs. (1) and (2) yields Eq. (3) for EE/O.

$$\mathrm{EE/O} = \frac{38.4 \times P}{Vk_a} \quad (3)$$

Most related studies compared efficiency using reaction rate constants. Few works considered the effects of power consumption [12,13]. Wu et al. [14] had plotted $\ln(A_i/A_o)$ against total energy consumption and determined the effective energy consumption constants (k_b, kJ^{-1}). Since the ozone reaction pathways depend strongly on the characteristics of the wastewater to be treated, including pH, promoters and scavengers in the solution, this study simultaneously employs k_a, EE/O and effective energy consumption constants, as proposed by Wu et al. [14], to evaluate the decolorization efficiency and power consumption of ozone-based systems at different pHs. The objectives of this investigation are (i) to calculate the k_a, k_b and EE/O values of ozone-based systems O_3, O_3/H_2O_2, O_3/Fe^{3+}, $O_3/H_2O_2/Fe^{3+}$, UV/O_3, $UV/O_3/Fe^{3+}$, $UV/O_3/H_2O_2$ and $UV/O_3/H_2O_2/Fe^{3+}$ systems at pH 4, 7 and 10; (ii) to clarify the effects of UV irradiation in these ozone-based systems; (iii) to determine the synergistic effects of different pHs and (iv) to compare the variations of k_a, k_b and EE/O with pH.

2. Materials and methods

2.1. Materials

The parent compound, RR2, obtained from Aldrich Chemical Company, was employed without further purification. The formula, molecular weight and maximum light absorption wavelength (λ_{max}) of RR2 were $C_{19}H_{10}Cl_2N_6Na_2O_7S_2$, 615 g/mol

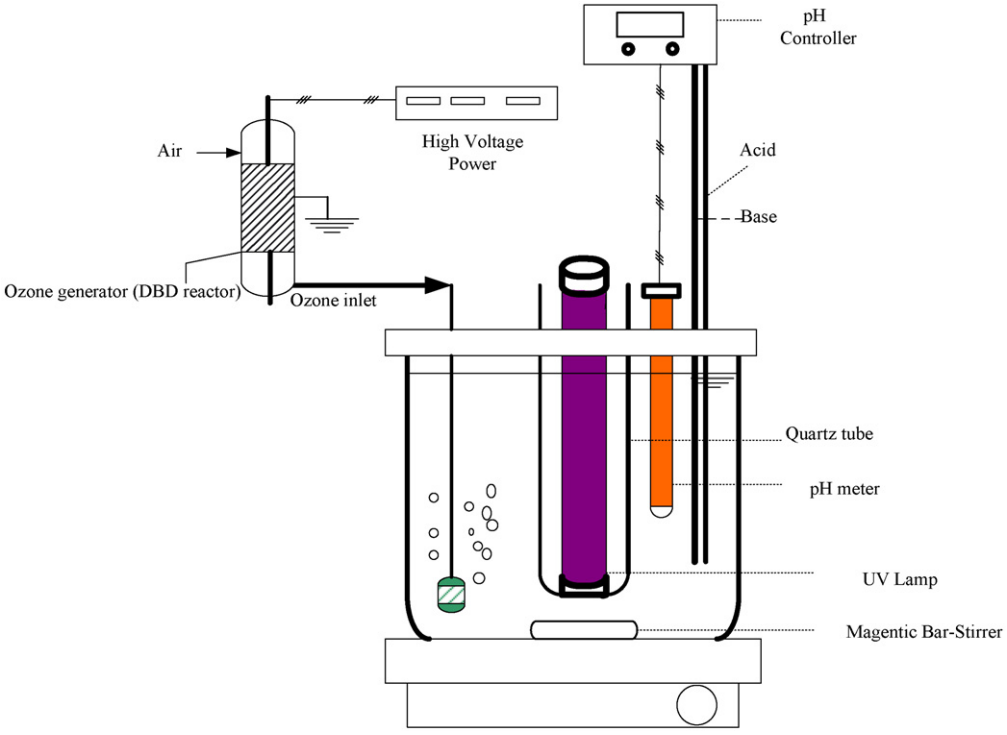

Fig. 1. Schematic diagram of the photoreactor (Wu and Chang [11]).

and 538 nm, respectively. The λ_{max} of RR2 did not vary with pH (data not shown for lack of space). Ferric sulfate ($Fe_2(SO_4)_3$) (Merck) was adopted as the supply of Fe^{3+}. Hydrogen peroxide solution (H_2O_2, 30%, w/w) was also provided by Merck. The solution pH was controlled by adding HNO_3 and NaOH via an automatic titrator. Other experimental chemicals were analytical grade. The water was deionized and doubly distilled with Milli-Q. A dielectric barrier discharge (DBD) reactor was applied to generate ozone, as was used by Wu and Chang [11]. The DBD reactor consumed the same power (8 W) at a gas flow rate of 500 ml/min. The schematic diagram of the photoreactor was presented in Fig. 1.

2.2. Decolorization experiments

The concentration of RR2 was 40 mg/l in all experiments. Decolorization experiments were conducted in a 3-l hollow cylindrical glass reactor. The inner diameter and height of the photoreactor were 143 and 230 mm, and those of the quartz tube were 36 and 210 mm, respectively. The inner tube was made of quartz, and in it was placed an 8 W, 254 nm UV-lamp (Philips) placed as the source of irradiation. The emission wavelength of the UV-lamp ranged from 230 to 320 nm. H_2O_2 was added to concentrations of 500, 1000, 3000, 5000 and 10,000 mg/l to determine the appropriate concentration of added H_2O_2 in the UV/H_2O_2 system. Fe^{3+} doses of 10, 25 and 50 mg/l were adopted to determine the optimal Fe^{3+} dosage in the UV/H_2O_2/Fe^{3+} system. All of the systems were stirred continuously at 300 rpm. A 15 ml aliquot was withdrawn from the photoreactor at prespecified intervals. The suspended solids were separated by centrifugation at 5000 rpm for 10 min, and then filtered through a 0.22 μm filter (Millipore). The decolorization of RR2 was detected using a spectrophotometer (HACH DR/4000U) at 538 nm and the decolorization ratio was calculated from the following equation.

$$\text{Decolorization ratio} = \frac{A_i - A_o}{A_i} \quad (4)$$

3. Results and discussion

3.1. Effects of Fe^{3+} and H_2O_2 dosage

The effects of H_2O_2 dosage at pH 7 in the UV/H_2O_2 system were evaluated at H_2O_2 500, 1000, 3000, 5000 and 10,000 mg/l. Eq. (5) specifies the reaction of the UV/H_2O_2 system.

$$H_2O_2 + h\nu \rightarrow 2OH^{\bullet} \quad (5)$$

The k_a values at 500, 1000, 3000, 5000 and 10,000 mg/l H_2O_2 in the UV/H_2O_2 system were 0.060, 0.068, 0.059, 0.043 and 0.025 min^{-1}, respectively. The degradation rate of organics normally increased as the H_2O_2 concentration increased until a critical H_2O_2 concentration was reached, because more hydroxyl radicals were formed as the H_2O_2 concentration increased (Eq. (5)). At high H_2O_2 concentration, competition exists between the substrate and H_2O_2. H_2O_2 at high concentration acts as a scavenger of hydroxyl radicals to generate perhydroxyl radicals, which have much lower oxidation capacities than hydroxyl radicals (Eq. (6)) [15–20]. Furthermore, the recombination of hydroxyl radicals also reduced the decolorization efficiency (Eq. (7)). As the H_2O_2 concentration in the UV/H_2O_2 system increased from 500 to 1000 mg/l, the decolorization efficiency increased, but above this range, no further improvement could be obtained. Therefore, experiments on the effects of Fe^{3+} dose were conducted at a H_2O_2 concentration of 1000 mg/l.

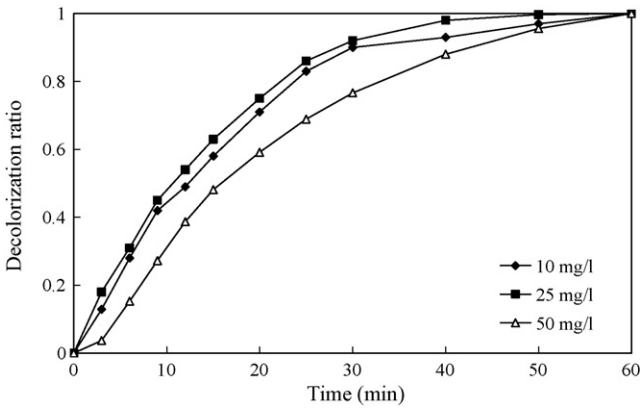

Fig. 2. Effects of Fe^{3+} dose in UV/H_2O_2/Fe^{3+} system (RR2 = 40 mg/l, H_2O_2 = 1000 mg/l, pH = 7 and T = 25 °C).

$$OH^{\bullet} + H_2O_2 \rightarrow HO_2^{\bullet} + H_2O \quad (6)$$

$$2OH^{\bullet} \rightarrow H_2O_2 \quad (7)$$

The amount of Fe^{3+} is one of the main parameters that affect the UV/H_2O_2/Fe^{3+} system. In this investigation, various concentrations of Fe^{3+} were utilized to determine its optimal original concentration. Fig. 2 plots the effect of Fe^{3+} dose in the UV/H_2O_2/Fe^{3+} system at pH 7. In the first 30 min, dye decolorization reached approximately 90%, 92% and 77% for Fe^{3+} doses of 10, 25 and 50 mg/l, respectively. The k_a values for 10, 25 and 50 mg/l Fe^{3+} in the UV/H_2O_2/Fe^{3+} system were 0.070, 0.072 and 0.046 min^{-1}, respectively. The effects of Fe^{3+} dose on dye decolorization were similar to that of H_2O_2. The reaction rate constants initially increased to a critical value and then declined [19]. When the Fe^{3+} concentration was high, Fe^{3+} underwent a reaction with hydroxyl ions to produce $Fe(OH)^{2+}$, which has strong UV absorption, reducing the intensity of the UV light [21]. Fig. 3 plots EE/O versus $[H_2O_2]_0/[dye]_0$ and $[Fe^{3+}]_0/[dye]_0$. The experimental results revealed that the energy efficiency was highest at $[H_2O_2]_0/[dye]_0 = 25$ ($[H_2O_2]_0$ = 1000 mg/l) and $[Fe^{3+}]_0/[dye]_0 = 0.625$ ($[Fe^{3+}]_0$ = 25 mg/l). Accordingly, the dosage of H_2O_2 and Fe^{3+} in the hybrid ozone-based systems was maintained at these values. Hydrogen peroxide/catalyst ratios from 10:1 to 40:1 are generally recommended as optimal in Fenton treatment [22,23]. The ratio 40:1 was adopted herein, agreeing with the recommendations made in earlier studies.

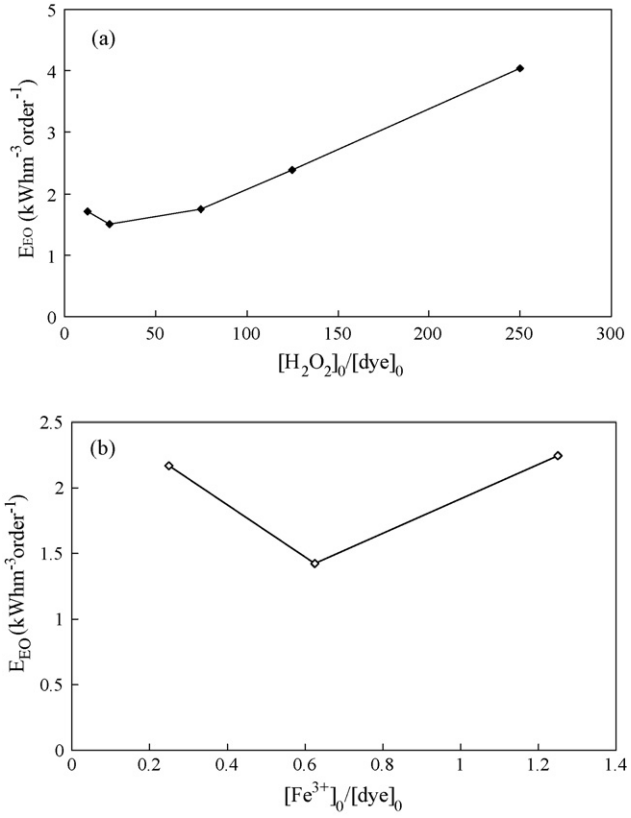

Fig. 3. Electrical energy per order as a function of $[H_2O_2]_0/[dye]_0$ and $[Fe^{3+}]_0/[dye]_0$ (a) $[H_2O_2]_0/[dye]_0$ and (b) $[Fe^{3+}]_0/[dye]_0$ (RR2 = 40 mg/l, pH = 7 and T = 25 °C).

3.2. Decolorization efficiency of ozone-based systems

Fig. 4 plots the decolorization curves of RR2 at different pH values in the group of experiments based on ozone. After 30 min of reaction, the decolorization ratios of the O_3, O_3/Fe^{3+}, O_3/H_2O_2 and $O_3/H_2O_2/Fe^{3+}$ systems at pH 4 were 56%, 72%, 27% and 92% (Fig. 4(a)); those at pH 7 were 77%, 73%, 49% and 63% (Fig. 4(b)), and those at pH 10 were 95%, 89%, 57% and 64% (Fig. 4(c)). Table 1 summarizes the pseudo-first-order reaction rate constants and correlation coefficients of various

Table 1
Pseudo-first-order reaction rate constants (k_a, min^{-1}) and correlation coefficients of various ozone-based systems

	pH 4		pH 7		pH 10	
	k_a	R^2	k_a	R^2	k_a	R^2
Non-UV systems						
O_3	0.028	0.983	0.049	0.976	0.096	0.996
O_3/Fe^{3+}	0.041	0.999	0.040	0.948	0.077	0.979
O_3/H_2O_2	0.011	0.987	0.024	0.994	0.029	0.990
$O_3/H_2O_2/Fe^{3+}$	0.074	0.956	0.034	0.994	0.035	0.988
With-UV systems						
UV/O_3	0.032	0.977	0.049	0.975	0.110	0.998
$UV/O_3/Fe^{3+}$	0.024	0.998	0.048	0.958	0.070	0.989
$UV/O_3/H_2O_2$	0.091	0.943	0.089	0.972	0.065	0.976
$UV/O_3/H_2O_2/Fe^{3+}$	0.209	0.973	0.096	0.976	0.069	0.984

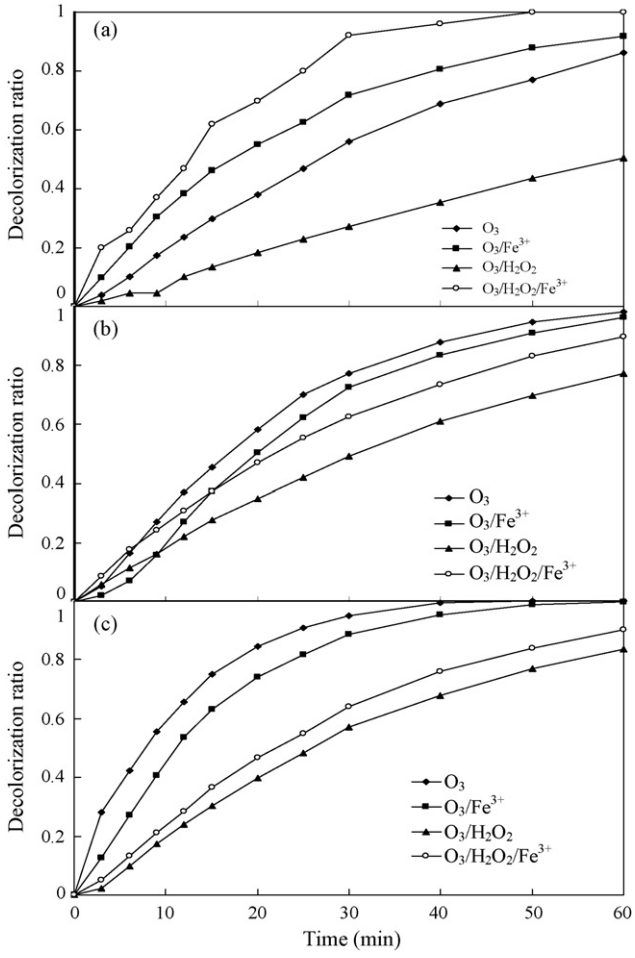

Fig. 4. Decolorization curves of RR2 in the group of experiments based on ozone (a) pH 4, (b) pH 7 and (c) pH 10 (RR2 = 40 mg/l, ozone flow rate = 500 ml/min, H_2O_2 = 1000 mg/l, Fe^{3+} = 25 mg/l and T = 25 °C).

ozone-based systems. Since all of the correlation coefficients of ozone-based systems exceed 0.92, the k_a values of ozone-based systems satisfy pseudo-first-order kinetics, and several works have shown that dye decolorization rates can generally be approximated using pseudo-first-order kinetics [4–6,8,11,19].

Ozone reacts with dyes either by electrophilic and/or nucleophilic addition (along a direct pathway) or indirectly by radical chain reactions, depending on the operating pH. The k_a values of O_3, O_3/Fe^{3+} and O_3/H_2O_2 systems were greater under alkaline than under acidic conditions (Table 1). Ozone oxidizes organics via two possible degradation pathways; (i) at basic pH, it rapidly decomposes to yield hydroxyl and other radical species in solution, according to Eqs. (8)–(10), and (ii) in acidic pH, ozone is stable and can react directly with organic substrates [24]. Since the oxidation potential of hydroxyl radicals significantly exceeds that of the ozone molecule, direct oxidation is slower than radical oxidation [1]. Alaton et al. [25] indicated that increasing the ozonation system pH increases the OH radical production rate. The decolorization rate increased with pH. Typically, at pH < 4, direct ozonation dominates, in the range of pH 4–9, both are important, and above pH > 9 the indirect pathway dominates [26]. The pH influences the generation of

hydroxyl radicals and thereby the decolorization efficiency.

$$O_3 + OH^- \rightarrow O_3^{-\bullet} + OH^\bullet \quad (8)$$

$$O_3^{-\bullet} \rightarrow O^{-\bullet} + O_2 \quad (9)$$

$$O^{-\bullet} + H^+ \rightarrow OH^\bullet \quad (10)$$

Unlike O_3, O_3/Fe^{3+} and O_3/H_2O_2 systems, the $O_3/H_2O_2/Fe^{3+}$ system had a higher k_a under acidic than under alkaline conditions. The experimental results implied that the dominant reactant in O_3, O_3/Fe^{3+} and O_3/H_2O_2 systems was O_3 and that in the $O_3/H_2O_2/Fe^{3+}$ system was H_2O_2/Fe^{3+}. The general mechanism of the H_2O_2/Fe^{3+} system (Fenton-like) involves numerous cyclic reactions. These ions are generated in their original state at the end of the cyclic reactions, based on the Eqs. (11) and (12) [4,17,27]. Hydroperoxyl and hydroxyl radicals will be generated from Fe^{3+} and Fe^{2+} according to Eqs. (11) and (12), respectively. However, hydroperoxyl radicals will be scavenged by Fe^{3+} in Eq. (13). In alkali, the Eqs. (11) and (13) are promoted and Eq. (12) is inhibited. Under alkaline conditions, the hydroperoxyl radicals that are additionally produced by Eq. (11) are nullified by Eq. (13), and the generation of hydroxyl radicals according to Eq. (12) will be inhibited. Additionally, H_2O_2 auto-decomposes to water and oxygen and Fe^{3+} precipitates to $Fe(OH)_3$ under alkaline conditions. Then, the cyclic reactions (Eqs. (11) and (12)) were interrupted and the decolorization ability finally eliminated. Hence, the $O_3/H_2O_2/Fe^{3+}$ system had a higher k_a value under acidic than under alkaline conditions.

$$Fe^{3+} + H_2O_2 \rightarrow Fe^{2+} + H^+ + HO_2^\bullet \quad (11)$$

$$Fe^{2+} + H_2O_2 \rightarrow Fe^{3+} + OH^- + OH^\bullet \quad (12)$$

$$Fe^{3+} + HO_2^\bullet \rightarrow Fe^{2+} + H^+ + O_2 \quad (13)$$

At pH 4, the k_a values of the ozone-based systems followed the order $O_3/H_2O_2/Fe^{3+} > O_3/Fe^{3+} > O_3 > O_3/H_2O_2$, at pH 7 and 10, the order was $O_3 > O_3/Fe^{3+} > O_3/H_2O_2/Fe^{3+} > O_3/H_2O_2$. Notably, O_3/H_2O_2 exhibited inhibitive effects under all experimental conditions; $O_3/H_2O_2/Fe^{3+}$ and O_3/Fe^{3+} had synergistic effects only under acidic conditions (Table 1). The inhibitive effects of O_3/H_2O_2 may contribute to the scavenging of H_2O_2, as mentioned in Eq. (6) [15–20]. Esplugas et al. [7] also presented an inhibitory effect in O_3/H_2O_2 at H_2O_2 concentrations of above 211 mg/l. When Fe^{3+} is incorporated into the O_3/H_2O_2 system, the scavenging effect of H_2O_2 is inhibited, since Fe^{3+} reacts with H_2O_2 (Eqs. (11) and (12)) to generate radicals, accelerating decolorization. Furthermore, O_3 and Fe^{3+} react to produce hydroxyl radicals, as described in Eq. (14) [28]. At a pH of above 4, the dissolved fraction of iron species declines as colloidal ferric species are formed [26]. Accordingly, $O_3/H_2O_2/Fe^{3+}$ and O_3/Fe^{3+} systems exhibited synergistic effects only under acidic conditions. Arslan [29] revealed that adding Fe^{2+} to the ozone system accelerated the oxidation kinetics at pH 3, which effect was similar to that of adding Fe^{3+} to an ozone system at pH 4 herein.

$$Fe^{3+} + O_3 \rightarrow FeO^{2+} + H^+ + O_2 + OH^\bullet \quad (14)$$

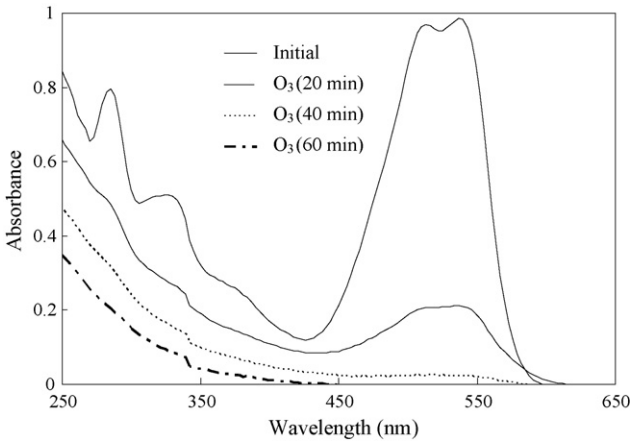

Fig. 5. UV–Vis absorption spectra of RR2 during decolorization with ozone (RR2 = 40 mg/l, ozone flow rate = 500 ml/min, pH = 7 and T = 25 °C).

Fig. 5 depicts the UV–Vis spectral changes of RR2 at pH 7 in the O_3 system. Before treatment, the UV–Vis spectra of RR2 consist of three main absorption bands: two are in UV region (285 and 330 nm) and one is in visible region (538 nm). The UV band is characteristic of two adjacent rings, while the visible band has a long conjugated π system that is linked by two azo groups [30]. The intensity of absorption in 538 nm disappears very fast (from 0.99 to 0.21) after 20 min. The UV bands at 285 nm (from 0.80 to 0.48) and 330 nm (from 0.51 to 0.27) were also observed to vanish after 20 min but at a lower rate than the visible band.

3.3. Decolorization efficiency of UV/ozone-based systems

Fig. 6(a–c) plot the decolorization curves of RR2 at pH 4, 7 and 10, respectively, in the group of experiments based on UV/ozone. After a 30 min reaction, the decolorization ratios of UV/O_3, $UV/O_3/Fe^{3+}$, $UV/O_3/H_2O_2$ and $UV/O_3/H_2O_2/Fe^{3+}$ systems at pH 4 were 60%, 51%, 97% and 100%; respectively, those at pH 7 were 78%, 79%, 97% and 96%, and those at pH 10 were 97%, 89%, 87% and 86%, respectively. The decolorization efficiency of RR2 is generally higher in UV/ozone-based systems than in ozone-based systems. The k_a values of UV/O_3 and $UV/O_3/Fe^{3+}$ systems were larger under alkaline than under acidic conditions, which result was similar to those in O_3 and O_3/Fe^{3+} systems. Furthermore, the k_a value of $O_3/H_2O_2/Fe^{3+}$ and $UV/O_3/H_2O_2/Fe^{3+}$ systems was highest under acidic conditions (Table 1). Notably, the k_a values of the $UV/O_3/H_2O_2$ system followed the order pH 4 > pH 7 > pH 10; in contrast, those of the O_3/H_2O_2 system obeyed followed order pH 10 > pH 7 > pH 4. The experimental results suggest that the dominant oxidant of the O_3/H_2O_2 system was O_3 and that of the $UV/O_3/H_2O_2$ system was H_2O_2.

At pH 4 and 7, the k_a values of the UV/ozone based systems followed the order $UV/O_3/H_2O_2/Fe^{3+} > UV/O_3/H_2O_2 > UV/O_3 > UV/O_3/Fe^{3+}$; at pH 10, the order was $UV/O_3 > UV/O_3/Fe^{3+} \geqq UV/O_3/H_2O_2/Fe^{3+} > UV/O_3/H_2O_2$ (Table 1). Combining ozone with UV promotes the degradation of dyes by the direct and indirect formation of hydroxyl

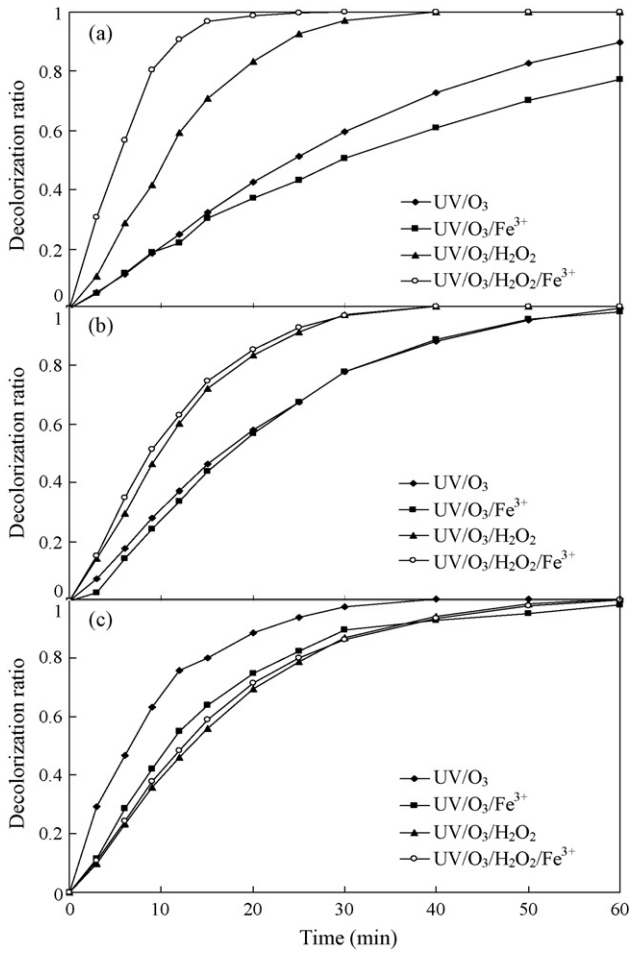

Fig. 6. Decolorization curves of RR2 in the group of experiments based on UV/ozone (a) pH 4, (b) pH 7 and (c) pH 10 (RR2 = 40 mg/l, ozone flow rate = 500 ml/min, H_2O_2 = 1000 mg/l, Fe^{3+} = 25 mg/l and T = 25 °C).

radicals, following ozone decomposition and hydrogen peroxide formation, respectively (Eqs. (5) and (15)) [31]. The combined process is more effective because UV radiation enhances ozone decomposition, yielding more hydroxyl radicals, thereby increasing the ozonation rate. Various works have also demonstrated that UV promotes ozone decolorization [10,11,14,31,32].

$$O_3 + H_2O + h\nu \rightarrow O_2 + H_2O_2 \quad (15)$$

Markedly, the O_3/H_2O_2 system has inhibitive effects; in contrast, the $UV/O_3/H_2O_2$ system has synergistic effects (Table 1). Since H_2O_2 does not have sufficient oxidation ability to decolorize dyes [4,27], and H_2O_2 scavenges hydroxyl radicals (Eq. (6)), inhibitive effects were observed in the O_3/H_2O_2 system. Combining UV with the O_3/H_2O_2 system can decompose H_2O_2 to produce hydroxyl radicals (Eq. (5)) and prevent the scavenging of H_2O_2, accelerating decolorization. The reaction in the UV/Fe^{3+} system is as stated in Eq. (16) [17,27]. However, $OH^\bullet$ might be scavenged by Fe^{2+} (Eq. (17)). Additionally, Fe^{3+} ions tend to form organic complexes, which inhibit the regeneration cycle of iron, indirectly causing a lack of hydroxyl radicals in solution [33]. Therefore, the synergistic effects were not observed in the $UV/O_3/Fe^{3+}$ system. Contreras et al. [9] also found that adding Fe^{3+} to the UV/O_3 system inhibited the degradation of nitrobenzene. Phenol degradation is faster with O_3 than with $UV/O_3/Fe^{3+}$ probably because the competition between reaction intermediates and ion species on one hand and phenol on the other hand for ozone present in the solution [34].

$$Fe^{3+} + H_2O + h\nu \rightarrow Fe^{2+} + H^+ + OH^\bullet \quad (16)$$

$$Fe^{2+} + OH^\bullet \rightarrow Fe^{3+} + OH^- \quad (17)$$

In the $UV/O_3/H_2O_2/Fe^{3+}$ system, hydroxyl radicals (Eqs. (5), (12), (14) and (16)) and hydroperoxyl radicals (Eq. (11)) were formed. Iron cycles between Fe^{3+} and Fe^{2+} under irradiation by light. The experimental results reveal that the decolorization rate of $UV/O_3/H_2O_2/Fe^{3+}$ exceeded that of $UV/O_3/H_2O_2$, which finding is similar to those elsewhere, which indicated that the reaction rates of photo-Fenton and photo-Fenton-like systems exceeds that of the UV/H_2O_2 system [2,4,35]. Beltran-Heredia et al. [2] added O_3 to $UV/H_2O_2/Fe^{2+}$ to degrade *p*-hydroxybenzoic acid and Dominguez et al. [4] incorporated O_3 into $UV/H_2O_2/Fe^{3+}$ to decolorize C.I. Acid Red 2. Both sets of results revealed that hybrid O_3/photo-Fenton and O_3/photo-Fenton-like systems had the highest reaction rates. These experimental results demonstrated that adding Fe^{3+} or H_2O_2/Fe^{3+} to O_3 at pH 4 and adding H_2O_2 or H_2O_2/Fe^{3+} into UV/O_3 at pH 4 and 7 yielded a higher decolorization rate than O_3 and UV/O_3, respectively.

3.4. Analyses of energy consumption efficiency

Fig. 7(a–c) plot the relationships between decolorization ratio and total energy consumption at pH 4, 7 and 10, respectively, for ozone- and UV/ozone-based systems. This study plots $\ln(A_i/A_o)$ against total energy consumption and determines the effective energy consumption constants (k_b). These values in ozone- and UV/ozone-based systems were found to be consistent with pseudo-first-order kinetics (Table 2). This investigation proposes that a higher k_b value corresponds to more efficient energy consumption during decolorization. The EE/O values were determined from Eq. (3) and higher EE/O values corresponded to the lower energy efficiency of the system (Table 2). Noticeably, k_a and k_b followed different trends at the same pH. The results imply that not all of the input energy is consumed in decolorization. At pH 4, the highest decolorization rate and the highest effective energy consumption constant (or the lowest EE/O value) were both found in the $UV/O_3/H_2O_2/Fe^{3+}$ system. However, at pH 10, the highest values of k_a and k_b were those of the UV/O_3 and O_3 system, respectively. At pH 4, the EE/O results indicated that the $UV/O_3/H_2O_2/Fe^{3+}$ system reduced 85% of the energy consumption compared with the UV/O_3 system. Moreover, the $O_3/H_2O_2/Fe^{3+}$ system reduced 62% of the energy consumption compared with the O_3 system. At pH 7, the EE/O results indicated that $UV/O_3/H_2O_2/Fe^{3+}$ system consumed half the energy consumed by the UV/O_3 system. Based on the analyses of decolorization efficiency and power consumption, this study suggested that the $UV/O_3/H_2O_2/Fe^{3+}$ system was effective in decolorizing RR2 at pH 4 and 7. Furthermore,

Table 2
Effective energy consumption constants (k_b, kJ^{-1}) and electrical energy per order (EE/O, kW h m^{-3} $order^{-1}$) of various ozone-based systems

	pH 4			pH 7			pH 10		
	k_b	R^2	EE/O	k_b	R^2	EE/O	k_b	R^2	EE/O
Non-UV systems									
O_3	0.058	0.983	3.684	0.109	0.970	2.111	0.199	0.996	1.070
O_3/Fe^{3+}	0.086	0.999	2.473	0.084	0.948	2.541	0.150	0.988	1.332
O_3/H_2O_2	0.023	0.987	9.225	0.049	0.994	4.321	0.060	0.990	3.568
$O_3/H_2O_2/Fe^{3+}$	0.154	0.956	1.384	0.073	0.990	3.030	0.075	0.986	2.968
With-UV systems									
UV/O_3	0.036	0.974	6.420	0.051	0.975	4.223	0.118	0.994	1.865
$UV/O_3/Fe^{3+}$	0.025	0.998	8.533	0.050	0.958	4.240	0.068	0.989	2.909
$UV/O_3/H_2O_2$	0.105	0.935	2.256	0.093	0.972	2.306	0.064	0.977	3.141
$UV/O_3/H_2O_2/Fe^{3+}$	0.234	0.968	0.979	0.108	0.968	2.133	0.072	0.984	2.972

UV/O_3 and O_3 systems were satisfactory for decolorizing RR2 at pH 10. Gutowska et al. [36] indicated that ozonation was more effective for C.I. Reactive Orange 113 degradation than for Fenton's process. However, Jozwiak et al. [37] demonstrated that Fenton's process was more effective than ozonation for C.I. Acid Brown 159. Additionally, the EE/O values were found to depend on the concentration of oxidant, the concentration and the basic structure of the dye [13]. Hence, this investigation suggests that the optimal conditions (both for decolorization efficiency and effective energy consumption) varied among the dyes, revealing that the development of a general decolorization method for a mixture of dyes would be very difficult.

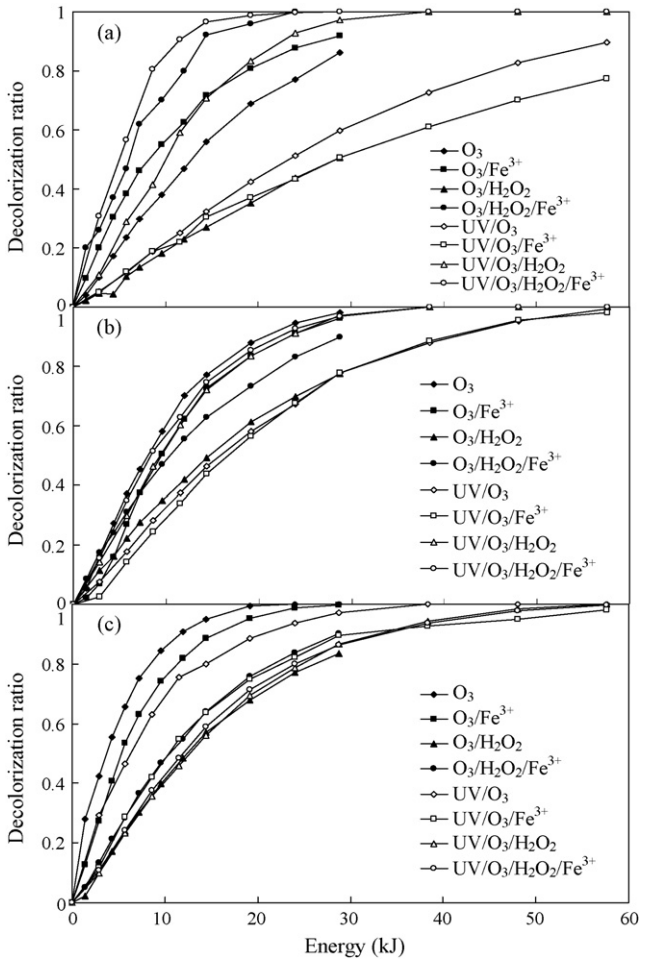

Fig. 7. Relationship between decolorization ratio and total energy consumption for ozone- and UV/ozone-based systems (a) pH 4, (b) pH 7 and (c) pH 10 (RR2 = 40 mg/l, ozone flow rate = 500 ml/min, H_2O_2 = 1000 mg/l, Fe^{3+} = 25 mg/l and T = 25 °C).

4. Conclusion

The decolorization rate constants, effective energy consumption constants and electrical energy per order of pollutant removal in O_3, O_3/H_2O_2, O_3/Fe^{3+}, $O_3/H_2O_2/Fe^{3+}$, UV/O_3, $UV/O_3/Fe^{3+}$, $UV/O_3/H_2O_2$ and $UV/O_3/H_2O_2/Fe^{3+}$ systems were determined at pH 4, 7 and 10. The effect of Fe^{3+} dose on dye decolorization was similar to that of H_2O_2; the reaction rate constants initially increased to a critical value and then declined. The k_a values of O_3, O_3/Fe^{3+}, O_3/H_2O_2, UV/O_3 and $UV/O_3/Fe^{3+}$ systems were larger under alkaline than under acidic conditions. However, $O_3/H_2O_2/Fe^{3+}$, $UV/O_3/H_2O_2$ and $UV/O_3/H_2O_2/Fe^{3+}$ systems varied oppositely. The experimental results indicated that the combination of Fe^{3+} or H_2O_2/Fe^{3+} into O_3 at pH 4 and H_2O_2 or H_2O_2/Fe^{3+} with UV/O_3 at pH 4 and 7 could yields a higher decolorization rate than O_3 and UV/O_3, respectively. The EE/O and k_b values followed the same order for both ozone- and UV/ozone-based systems. Based on the analyses of decolorization efficiency and power consumption, this study suggests that the $UV/O_3/H_2O_2/Fe^{3+}$ system was an appropriate method for decolorizing RR2 at pH 4 and 7. Moreover, UV/O_3 and O_3 systems are acceptable for decolorizing RR2 at pH 10.

Acknowledgement

The authors would like to thank the National Science Council of the Republic of China for financially supporting this research under Contract No. NSC 95-2221-E-212-022.

References

[1] E. Oguz, B. Keskinler, Z. Celik, Ozonation of aqueous Bomaplex Red CR-L dye in a semi-batch reactor, Dyes Pigments 64 (2005) 101–108.

[2] J. Beltran-Heredia, J. Torregrosa, J.R. Dominguez, J.A. Peres, Comparison of the degradation of *p*-hydroxybenzoic acid in aqueous solution by several oxidation processes, Chemosphere 42 (2001) 351–359.
[3] T. Kurbus, A.M.L. Marechal, D.B. Voncina, Comparison of H_2O_2/UV, H_2O_2/O_3 and H_2O_2/Fe^{2+} processes for the decolorisation of vinylsulphone reactive dyes, Dyes Pigments 58 (2003) 245–252.
[4] J.R. Dominguez, J. Beltran, O. Rodriguez, Vis and UV photocatalytic detoxification methods (using TiO_2, TiO_2/H_2O_2, TiO_2/O_3, $TiO_2/S_2O_8^{2-}$, O_3, H_2O_2, $S_2O_8^{2-}$, Fe^{3+}/H_2O_2 and $Fe^{3+}/H_2O_2/C_2O_4^{2-}$) for dyes treatment, Catal. Today 101 (2005) 389–395.
[5] E. Brillas, J.C. Calpe, P.L. Cabot, Degradation of the herbicide 2,4-dichlorophenoxyacetic acid by ozonation catalyzed with Fe^{2+} and UVA light, Appl. Catal. B: Environ. 46 (2003) 381–391.
[6] M. Skoumal, P.L. Cabot, F. Centellas, C. Arias, R.M. Rodriguez, J.A. Garrido, E. Brillas, Mineralization of paracetamol by ozonation catalyzed with Fe^{2+}, Cu^{2+}, and UVA light, Appl. Catal. B: Environ. 66 (2006) 228–240.
[7] S. Esplugas, J. Gimenez, S. Contreras, E. Pascual, M. Rodriguez, Comparison of different advanced oxidation processes for phenol degradation, Water Res. 36 (2002) 1034–1042.
[8] E. Brillas, P.L. Cabot, R.M. Rodriguez, C. Arias, J.A. Garrido, R. Oliver, Degradation of the herbicide 2,4-DP by catalyzed ozonation using the O_3/Fe^{2+}/UVA system, Appl. Catal. B: Environ. 51 (2004) 117–127.
[9] S. Contreras, M. Rodriguez, E. Chamarro, S. Esplugas, UV- and UV/Fe(III)-enhanced ozonation in aqueous solution, J. Photochem. Photobiol., A: Chem. 142 (2001) 79–83.
[10] C.H. Wu, C.L. Chang, C.Y. Kuo, Decolorization of Amaranth by advanced oxidation processes, React. Kinet. Catal. Lett. 86 (2005) 37–43.
[11] C.H. Wu, C.L. Chang, Decolorization of Procion Red MX-5B by advanced oxidation processes: comparative studies of the homogeneous and heterogeneous systems, J. Hazard. Mater. 128 (2006) 265–272.
[12] J.R. Bolton, K.G. Bircger, W. Tumas, C.A. Tolman, Figure-of merit for the technical development and application of advanced oxidation technologies for both electric- and solar-derived systems, Pure Appl. Chem. 73 (2001) 627–637.
[13] N. Daneshvar, A. Aleboyeh, A.R. Khataee, The evaluation of electrical energy per order (E_{EO}) for photooxidative decolorization of four textile dye solutions by the kinetic model, Chemosphere 59 (2005) 761–767.
[14] C.H. Wu, C.L. Chang, C.Y. Kuo, Decolorization of Procion Red MX-5B in electrocoagulation (EC), UV/TiO_2 and ozone related systems, Dyes Pigments 76 (2008) 187–194.
[15] M.Y. Ghaly, G. Hartel, R. Mayer, R. Haseneder, Photochemical oxidation of *p*-chlorophenol by UV/H_2O_2 and photo-Fenton process. A comparative study, Waste Manage. 21 (2001) 41–47.
[16] H. Kusic, N. Koprivanac, L. Srsan, Azo dye degradation using Fenton type processes assisted by UV irradiation: a kinetic study, J. Photochem. Photobiol., A-Chem. 181 (2006) 195–202.
[17] H. Kusic, N. Koprivanac, A.L. Bozic, I. Selanec, Photo-assisted Fenton type processes for the degradation of phenol: a kinetic study, J. Hazard. Mater. 136 (2006) 632–644.
[18] M. Tokumura, A. Ohta, H.T. Znad, Y. Kawase, UV light assisted decolorization of dark brown colored coffee effluent by photo-Fenton reaction, Water Res. 40 (2006) 3775–3784.
[19] M.M. Alnuaimi, M.A. Rauf, S.S. Ashraf, Comparative decoloration study of Neutral Red by different oxidative processes, Dyes Pigments 72 (2007) 367–371.
[20] N. Modirshahla, M.A. Behnajady, F. Ghanbary, Decolorization and mineralization of C.I. Acid Yellow 23 by Fenton and photo-Fenton processes, Dyes Pigments 73 (2007) 305–310.
[21] M.P. Titus, V.G. Molina, M.A. Banos, J. Gimenez, S. Esplugas, Degradation of chlorophenols by means of advanced oxidation processes: a general review, Appl. Catal. B: Environ. 47 (2004) 219–256.
[22] G. Ruppert, R. Bauer, G. Heisler, UV-O_3, UV-H_2O_2, UV-TiO_2 and photo-Fenton – comparison of advanced oxidation processes for wastewater treatment, Chemosphere 28 (1994) 1447–1454.
[23] W.Z. Tang, P. Huang, Stoichiometry of Fenton's reagent in the oxidation of chlorinated aliphatic organic pollutants, Environ. Technol. 18 (1997) 13–23.
[24] W.H. Glaze, J.W. Kang, D.H. Chapin, The chemistry of water treatment processes involving ozone, hydrogen, and ultraviolet radiation, Ozone Sci. Eng. 9 (1987) 335–352.
[25] I.A. Alaton, I.A. Balcioglu, D.W. Bahnemann, Advanced oxidation of a reactive dyebath effluent: comparison of O_3, H_2O_2/UV-C and TiO_2/UV-A processes, Water Res. 36 (2002) 1143–1154.
[26] M. Pera-Titus, V. Garcia-Molina, M.A. Banos, J. Gimenez, S. Esplugas, Degradation of chlorophenols by means of advanced oxidation processes: a general review, Appl. Catal. B: Environ. 47 (2004) 219–256.
[27] S. Lucas, J.A. Peres, Decolorization of the azo dye Reactive Black 5 by Fenton and photo-Fenton oxidation, Dyes Pigments 71 (2006) 236–244.
[28] F.J. Beltran, F.J. Rivas, R. Montero-de-Espinosa, Iron type catalysts for the ozonation of oxalic acid in water, Water Res. 39 (2005) 3553–3564.
[29] I. Arslan, Treatability of a simulated disperse dye-bath by ferrous iron coagulation, ozonation, and ferrous iron-catalyzed ozonation, J. Hazard. Mater. 85 (2001) 229–241.
[30] R.M.C. Silverstein, G.C. Basdler, G.C. Morrill, Spectrophotometric Identification of Organic Compounds, Wiley, New York, 1991.
[31] G.R. Peyton, W.H. Glaze, The mechanism of photolytic ozonation, Abstr. Pap. Am. Chem. Soc. 189 (1985) 5.
[32] G. Tezcanli-Guyer, N.H. Ince, Individual and combined effects of ultrasound ozone and UV irradiation: a case study with textile dyes, Ultrasonics 42 (2004) 603–609.
[33] V. Kavitha, K. Palanivelu, The role of ferrous ion in Fenton and photo-Fenton processes for the degradation of phenol, Chemosphere 55 (2004) 1235–1243.
[34] C. Canton, S. Esplugas, J. Casado, Mineralization of phenol in aqueous solution by ozonation using iron or copper salts and light, Appl. Catal. B: Environ. 43 (2003) 139–149.
[35] M. Muruganandham, M. Swaminathan, Advanced oxidative decolourisation of Reactive Yellow 14 azo dye by UV/TiO_2, UV/H_2O_2, UV/H_2O_2/Fe^{2+} processes – a comparative study, Sep. Purif. Technol. 48 (2006) 297–303.
[36] A. Gutowska, J. Kaluzna-Czaplinska, W.K. Jozwiak, Degradation mechanism of Reactive Orange 113 dye by H_2O_2/Fe^{2+} and ozone in aqueous solution, Dyes Pigments 74 (2007) 41–46.
[37] W.K. Jozwiak, M. Mitros, J. Kaluzna-Czaplinska, R. Tosik, Oxidative decomposition of Acid Brown 159 dye in aqueous solution by H_2O_2/Fe^{2+} and ozone with GC/MS analysis, Dyes Pigments 74 (2007) 9–16.